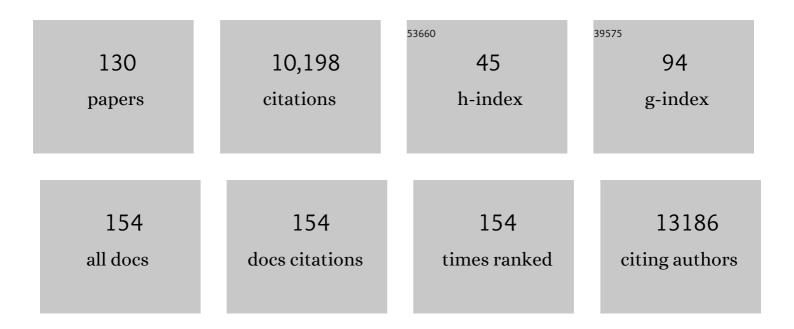
## Vladimir S Fonov

List of Publications by Year in descending order

Source: https://exaly.com/author-pdf/8809811/publications.pdf Version: 2024-02-01



#	Article	IF	CITATIONS
1	Unbiased average age-appropriate atlases for pediatric studies. Neurolmage, 2011, 54, 313-327.	2.1	1,825
2	Early brain development in infants at high risk for autism spectrum disorder. Nature, 2017, 542, 348-351.	13.7	808
3	Patch-based segmentation using expert priors: Application to hippocampus and ventricle segmentation. Neurolmage, 2011, 54, 940-954.	2.1	692
4	BEaST: Brain extraction based on nonlocal segmentation technique. NeuroImage, 2012, 59, 2362-2373.	2.1	507
5	SCT: Spinal Cord Toolbox, an open-source software for processing spinal cord MRI data. NeuroImage, 2017, 145, 24-43.	2.1	390
6	Standardized evaluation of algorithms for computer-aided diagnosis of dementia based on structural MRI: The CADDementia challenge. NeuroImage, 2015, 111, 562-579.	2.1	266
7	Prediction of Alzheimer's disease in subjects with mild cognitive impairment from the ADNI cohort using patterns of cortical thinning. NeuroImage, 2013, 65, 511-521.	2.1	224
8	Non-local MRI upsampling. Medical Image Analysis, 2010, 14, 784-792.	7.0	218
9	Network connectivity determines cortical thinning in early Parkinson's disease progression. Nature Communications, 2018, 9, 12.	5.8	198
10	Network structure of brain atrophy in de novo Parkinson's disease. ELife, 2015, 4, .	2.8	187
11	Increased Extra-axial Cerebrospinal Fluid in High-Risk Infants Who Later Develop Autism. Biological Psychiatry, 2017, 82, 186-193.	0.7	173
12	Anxious/Depressed Symptoms are Linked to Right Ventromedial Prefrontal Cortical Thickness Maturation in Healthy Children and Young Adults. Cerebral Cortex, 2014, 24, 2941-2950.	1.6	149
13	A new method for structural volume analysis of longitudinal brain MRI data and its application in studying the growth trajectories of anatomical brain structures in childhood. NeuroImage, 2013, 82, 393-402.	2.1	145
14	PAM50: Unbiased multimodal template of the brainstem and spinal cord aligned with the ICBM152 space. NeuroImage, 2018, 165, 170-179.	2.1	143
15	Benchmark on Automatic Six-Month-Old Infant Brain Segmentation Algorithms: The iSeg-2017 Challenge. IEEE Transactions on Medical Imaging, 2019, 38, 2219-2230.	5.4	136
16	CERES: A new cerebellum lobule segmentation method. NeuroImage, 2017, 147, 916-924.	2.1	133
17	The effect of template choice on morphometric analysis of pediatric brain data. NeuroImage, 2009, 45, 769-777.	2.1	131
18	Simultaneous segmentation and grading of anatomical structures for patient's classification: Application to Alzheimer's disease. NeuroImage, 2012, 59, 3736-3747.	2.1	129

#	Article	IF	CITATIONS
19	A comparison of publicly available linear MRI stereotaxic registration techniques. NeuroImage, 2018, 174, 191-200.	2.1	120
20	Neural circuitry at age 6Âmonths associated with later repetitive behavior and sensory responsiveness in autism. Molecular Autism, 2017, 8, 8.	2.6	111
21	Onset of multiple sclerosis before adulthood leads to failure of age-expected brain growth. Neurology, 2014, 83, 2140-2146.	1.5	107
22	Scoring by nonlocal image patch estimator for early detection of Alzheimer's disease. NeuroImage: Clinical, 2012, 1, 141-152.	1.4	104
23	Childhood cognitive ability accounts for associations between cognitive ability and brain cortical thickness in old age. Molecular Psychiatry, 2014, 19, 555-559.	4.1	104
24	Structural imaging biomarkers of Alzheimer's disease: predicting disease progression. Neurobiology of Aging, 2015, 36, S23-S31.	1.5	101
25	The Canadian Dementia Imaging Protocol: Harmonizing National Cohorts. Journal of Magnetic Resonance Imaging, 2019, 49, 456-465.	1.9	101
26	A dataset of multi-contrast population-averaged brain MRI atlases of a Parkinson׳s disease cohort. Data in Brief, 2017, 12, 370-379.	0.5	94
27	The Emergence of Network Inefficiencies in Infants With Autism Spectrum Disorder. Biological Psychiatry, 2017, 82, 176-185.	0.7	93
28	Framework for integrated MRI average of the spinal cord white and gray matter: The MNI–Poly–AMU template. NeuroImage, 2014, 102, 817-827.	2.1	92
29	Validation of a Regression Technique for Segmentation of White Matter Hyperintensities in Alzheimer's Disease. IEEE Transactions on Medical Imaging, 2017, 36, 1758-1768.	5.4	85
30	Identifying incipient dementia individuals using machine learning and amyloid imaging. Neurobiology of Aging, 2017, 59, 80-90.	1.5	85
31	Reduced head and brain size for age and disproportionately smaller thalami in child-onset MS. Neurology, 2012, 78, 194-201.	1.5	80
32	Comparing fully automated state-of-the-art cerebellum parcellation from magnetic resonance images. NeuroImage, 2018, 183, 150-172.	2.1	80
33	Performance comparison of 10 different classification techniques in segmenting white matter hyperintensities in aging. Neurolmage, 2017, 157, 233-249.	2.1	79
34	Jacobian integration method increases the statistical power to measure gray matter atrophy in multiple sclerosis. NeuroImage: Clinical, 2014, 4, 10-17.	1.4	73
35	VoxelStats: A MATLAB Package for Multi-Modal Voxel-Wise Brain Image Analysis. Frontiers in Neuroinformatics, 2016, 10, 20.	1.3	73
36	Regional brain atrophy in children with multiple sclerosis. NeuroImage, 2011, 58, 409-415.	2.1	71

#	Article	IF	CITATIONS
37	Subcortical Brain and Behavior Phenotypes Differentiate Infants With Autism Versus Language Delay. Biological Psychiatry: Cognitive Neuroscience and Neuroimaging, 2017, 2, 664-672.	1.1	71
38	Gradient distortions in MRI: Characterizing and correcting for their effects on SIENA-generated measures of brain volume change. NeuroImage, 2010, 49, 1601-1611.	2.1	68
39	Multi-contrast unbiased MRI atlas of a Parkinson's disease population. International Journal of Computer Assisted Radiology and Surgery, 2015, 10, 329-341.	1.7	68
40	MINC 2.0: A Flexible Format for Multi-Modal Images. Frontiers in Neuroinformatics, 2016, 10, 35.	1.3	65
41	Assessing atrophy measurement techniques in dementia: Results from the MIRIAD atrophy challenge. NeuroImage, 2015, 123, 149-164.	2.1	63
42	A stereotaxic, population-averaged T1w ovine brain atlas including cerebral morphology and tissue volumes. Frontiers in Neuroanatomy, 2015, 9, 69.	0.9	59
43	Automated segmentation of basal ganglia and deep brain structures in MRI of Parkinson's disease. International Journal of Computer Assisted Radiology and Surgery, 2013, 8, 99-110.	1.7	57
44	Rotation-invariant multi-contrast non-local means for MS lesion segmentation. NeuroImage: Clinical, 2015, 8, 376-389.	1.4	56
45	Detection of Alzheimer's disease signature in MR images seven years before conversion to dementia: Toward an early individual prognosis. Human Brain Mapping, 2015, 36, 4758-4770.	1.9	52
46	Accurate age classification of 6 and 12 month-old infants based on resting-state functional connectivity magnetic resonance imaging data. Developmental Cognitive Neuroscience, 2015, 12, 123-133.	1.9	51
47	Unbiased age-specific structural brain atlases for Chinese pediatric population. NeuroImage, 2019, 189, 55-70.	2.1	50
48	A longitudinal study of parentâ€reported sensory responsiveness in toddlers atâ€risk for autism. Journal of Child Psychology and Psychiatry and Allied Disciplines, 2019, 60, 314-324.	3.1	50
49	Nonrigid Registration of Ultrasound and MRI Using Contextual Conditioned Mutual Information. IEEE Transactions on Medical Imaging, 2014, 33, 708-725.	5.4	48
50	Dissociation between Brain Amyloid Deposition and Metabolism in Early Mild Cognitive Impairment. PLoS ONE, 2012, 7, e47905.	1.1	47
51	Sex-specific associations of testosterone with prefrontal-hippocampal development and executive function. Psychoneuroendocrinology, 2017, 76, 206-217.	1.3	44
52	Multimodal Imaging in Rat Model Recapitulates Alzheimer's Disease Biomarkers Abnormalities. Journal of Neuroscience, 2017, 37, 12263-12271.	1.7	44
53	Rapid automatic segmentation of the human cerebellum and its lobules (RASCAL)—Implementation and application of the patchâ€based labelâ€fusion technique with a template library to segment the human cerebellum. Human Brain Mapping, 2014, 35, 5026-5039.	1.9	43
54	Monophasic demyelination reduces brain growth in children. Neurology, 2017, 88, 1744-1750.	1.5	43

#	Article	IF	CITATIONS
55	CerebrA, registration and manual label correction of Mindboggle-101 atlas for MNI-ICBM152 template. Scientific Data, 2020, 7, 237.	2.4	43
56	Subjective Cognitive Decline Is Associated With Altered Default Mode Network Connectivity in Individuals With a Family History of Alzheimer's Disease. Biological Psychiatry: Cognitive Neuroscience and Neuroimaging, 2018, 3, 463-472.	1.1	41
57	Comparing two approaches to rigid registration of three-dimensional ultrasound and magnetic resonance images for neurosurgery. International Journal of Computer Assisted Radiology and Surgery, 2012, 7, 125-136.	1.7	39
58	Callosal fiber length and interhemispheric connectivity in adults with autism: Brain overgrowth and underconnectivity. Human Brain Mapping, 2013, 34, 1685-1695.	1.9	38
59	Contribution of the cerebellum to cognitive performance in children and adolescents with multiple sclerosis Journal, 2016, 22, 599-607.	1.4	38
60	The development of optical techniques for the measurement of pressure and skin friction. Measurement Science and Technology, 2006, 17, 1261-1268.	1.4	37
61	Morphometric Changes of the Corpus Callosum in Congenital Blindness. PLoS ONE, 2014, 9, e107871.	1.1	37
62	Resting State Executive Control Network Adaptations in Amnestic Mild Cognitive Impairment. Journal of Alzheimer's Disease, 2014, 40, 993-1004.	1.2	36
63	Splenium development and early spoken language in human infants. Developmental Science, 2017, 20, e12360.	1.3	36
64	Nonlocal Patch-Based Label Fusion for Hippocampus Segmentation. Lecture Notes in Computer Science, 2010, 13, 129-136.	1.0	36
65	A comparison of accurate automatic hippocampal segmentation methods. NeuroImage, 2017, 155, 383-393.	2.1	35
66	Development of cortical shape in the human brain from 6 to 24months of age via a novel measure of shape complexity. Neurolmage, 2016, 135, 163-176.	2.1	33
67	Neuroanatomical correlates of behavioral rating versus performance measures of working memory in typically developing children and adolescents Neuropsychology, 2015, 29, 82-91.	1.0	30
68	Test-retest resting-state fMRI in healthy elderly persons with a family history of Alzheimer's disease. Scientific Data, 2015, 2, 150043.	2.4	30
69	Adaptive prior probability and spatial temporal intensity change estimation for segmentation of the one-year-old human brain. Journal of Neuroscience Methods, 2013, 212, 43-55.	1.3	29
70	White Matter Abnormalities and Structural Hippocampal Disconnections in Amnestic Mild Cognitive Impairment and Alzheimer's Disease. PLoS ONE, 2013, 8, e74776.	1.1	28
71	Cyberinfrastructure for Open Science at the Montreal Neurological Institute. Frontiers in Neuroinformatics, 2016, 10, 53.	1.3	28
72	Dehydroepiandrosterone impacts working memory by shaping cortico-hippocampal structural covariance during development. Psychoneuroendocrinology, 2017, 86, 110-121.	1.3	27

#	Article	IF	CITATIONS
73	Cortical and subcortical T1 white/gray contrast, chronological age, and cognitive performance. NeuroImage, 2019, 196, 276-288.	2.1	25
74	Newborn amygdalar volumes are associated with maternal prenatal psychological distress in a sex-dependent way. NeuroImage: Clinical, 2020, 28, 102380.	1.4	25
75	The developmental relationship between DHEA and visual attention is mediated by structural plasticity of cortico-amygdalar networks. Psychoneuroendocrinology, 2016, 70, 122-133.	1.3	23
76	White matter microstructure is associated with hyperactive/inattentive symptomatology and polygenic risk for attention-deficit/hyperactivity disorder in a population-based sample of adolescents. Neuropsychopharmacology, 2019, 44, 1597-1603.	2.8	22
77	Impaired growth of the cerebellum in pediatric-onset acquired CNS demyelinating disease. Multiple Sclerosis Journal, 2016, 22, 1266-1278.	1.4	21
78	Accurate and robust segmentation of neuroanatomy in T1â€weighted MRI by combining spatial priors with deep convolutional neural networks. Human Brain Mapping, 2020, 41, 309-327.	1.9	21
79	Automated Analysis of Multi Site MRI Phantom Data for the NIHPD Project. Lecture Notes in Computer Science, 2006, 9, 144-151.	1.0	20
80	Non-Local Means Inpainting of MS Lesions in Longitudinal Image Processing. Frontiers in Neuroscience, 2015, 9, 456.	1.4	19
81	Patch-based label fusion segmentation of brainstem structures with dual-contrast MRI for Parkinson's disease. International Journal of Computer Assisted Radiology and Surgery, 2015, 10, 1029-1041.	1.7	17
82	MRI and cognitive scores complement each other to accurately predict Alzheimer's dementia 2 to 7 years before clinical onset. NeuroImage: Clinical, 2020, 25, 102121.	1.4	16
83	Improved Precision in the Measurement of Longitudinal Global and Regional Volumetric Changes via a Novel MRI Gradient Distortion Characterization and Correction Technique. Lecture Notes in Computer Science, 2010, , 324-333.	1.0	15
84	Human Brain Myelination from Birth to 4.5 Years. Lecture Notes in Computer Science, 2008, 11, 180-187.	1.0	14
85	White matter degeneration profile in the cognitive corticoâ€subcortical tracts in Parkinson's disease. Movement Disorders, 2018, 33, 1139-1150.	2.2	11
86	Detection and clinical correlation of leukocortical lesions in pediatric-onset multiple sclerosis on multi-contrast MRI. Multiple Sclerosis Journal, 2019, 25, 980-986.	1.4	11
87	Brain volume loss in individuals over time: Source of variance and limits of detectability. NeuroImage, 2020, 214, 116737.	2.1	11
88	Interhemispheric coupling improves the brain's ability to perform low cognitive demand tasks in Alzheimer's disease and high cognitive demand tasks in normal aging Neuropsychology, 2013, 27, 464-480.	1.0	10
89	Sexâ€specific association between infant caudate volumes and a polygenic risk score for major depressive disorder. Journal of Neuroscience Research, 2020, 98, 2529-2540.	1.3	10
90	A sub+cortical fMRlâ€based surface parcellation. Human Brain Mapping, 2022, 43, 616-632.	1.9	10

Vladimir S Fonov

#	Article	IF	CITATIONS
91	Developmental trajectories of neuroanatomical alterations associated with the 16p11.2 Copy Number Variations. NeuroImage, 2019, 203, 116155.	2.1	9
92	Simultaneous Segmentation and Grading of Hippocampus for Patient Classification with Alzheimer's Disease. Lecture Notes in Computer Science, 2011, 14, 149-157.	1.0	9
93	Spatio-Temporal Regularization for Longitudinal Registration to Subject-Specific 3d Template. PLoS ONE, 2015, 10, e0133352.	1.1	9
94	Lift and Drag Characteristics of a Blended-Wing Body Aircraft. Journal of Aircraft, 2007, 44, 1409-1421.	1.7	8
95	Regional Cerebellar Volume Loss Predicts Future Disability in Multiple Sclerosis Patients. Cerebellum, 2022, 21, 632-646.	1.4	8
96	A voxel-wise assessment of growth differences in infants developing autism spectrum disorder. NeuroImage: Clinical, 2021, 29, 102551.	1.4	8
97	Towards Automatic Collateral Circulation Score Evaluation in Ischemic Stroke Using Image Decompositions and Support Vector Machines. Lecture Notes in Computer Science, 2017, , 158-167.	1.0	7
98	The EADC-ADNI harmonized protocol for hippocampal segmentation: AÂvalidation study. NeuroImage, 2018, 181, 142-148.	2.1	7
99	DARQ: Deep learning of quality control for stereotaxic registration of human brain MRI to the T1w MNI-ICBM 152 template. NeuroImage, 2022, 257, 119266.	2.1	7
100	A new template to study callosal growth shows specific growth in anterior and posterior regions of the corpus callosum in early childhood. European Journal of Neuroscience, 2015, 42, 1675-1684.	1.2	6
101	MRI of Capn15 Knockout Mice and Analysis of Capn 15 Distribution Reveal Possible Roles in Brain Development and Plasticity. Neuroscience, 2021, 465, 128-141.	1.1	6
102	Allometry in the corpus callosum in neonates: Sexual dimorphism. Human Brain Mapping, 0, , .	1.9	6
103	An augmented-reality system prototype for guiding transcranial Doppler ultrasound examination. Multimedia Tools and Applications, 2018, 77, 27789-27805.	2.6	5
104	Amygdalar reactivity is associated with prefrontal cortical thickness in a large population-based sample of adolescents. PLoS ONE, 2019, 14, e0216152.	1.1	5
105	Neonatal amygdala volumes and the development of self-regulation from early infancy to	1.0	5
106	MNI-FTD templates, unbiased average templates of frontotemporal dementia variants. Scientific Data, 2021, 8, 222.	2.4	5
107	Rigid Registration of 3D Ultrasound and MRI: Comparing Two Approaches on Nine Tumor Cases. Advances in Intelligent and Soft Computing, 2010, , 33-43.	0.2	5
108	Using Surface Stress Sensitive Films for Pressure and Friction Measurements in Mini- and Mirro Chappels 2007		4

Micro-Channels. , 2007, , .

Vladimir S Fonov

#	Article	IF	CITATIONS
109	Atlas-based clustering of sulcal patterns — Application to the left inferior frontal sulcus. , 2012, , .		4
110	Spatial intensity prior correction for tissue segmentation in the developing human brain. , 2011, , 2049-2052.		2
111	IC-P-150: A UNIFIED ASSESSMENT OF FULLY AUTOMATED HIPPOCAMPUS SEGMENTATION METHODS. , 2014, 10 P86-P86.	,	2
112	Shape index distribution based local surface complexity applied to the human cortex. Proceedings of SPIE, 2015, 9413, .	0.8	2
113	Ageâ€specific associations between oestradiol, corticoâ€amygdalar structural covariance, and verbal and spatial skills. Journal of Neuroendocrinology, 2019, 31, e12698.	1.2	2
114	A novel framework for the local extraction of extra-axial cerebrospinal fluid from MR brain images. , 2018, 10574, .		2
115	Measurements of Non-Steady Pressure and Skin Friction Fields on Wall Mounted Cube Using Surface Stress Sensitive Film. , 2007, , .		1
116	ICâ€Pâ€099: A quantitative comparison between two manual hippocampal segmentation protocols. Alzheimer's and Dementia, 2015, 11, P67.	0.4	1
117	IC-P-012: Should a global or a regional measure of amyloidosis be used in a longitudinal study?. , 2015, 11, P19-P19.		1
118	Is It Possible to Differentiate the Impact of Pediatric Monophasic Demyelinating Disorders and Multiple Sclerosis After a First Episode of Demyelination?. Lecture Notes in Computer Science, 2015, , 38-48.	1.0	1
119	Atlas-Guided Transcranial Doppler Ultrasound Examination with a Neuro-Surgical Navigation System: Case Study. Lecture Notes in Computer Science, 2016, , 19-27.	1.0	1
120	Spatio-temporal Regularization for Longitudinal Registration to an Unbiased 3D Individual Template. Lecture Notes in Computer Science, 2012, , 1-12.	1.0	1
121	Sex-specific associations between maternal pregnancy-specific anxiety and newborn amygdalar volumes - preliminary findings from the FinnBrain Birth Cohort Study. Stress, 2022, 25, 213-226.	0.8	1
122	Increased brain volumetric measurement precision from multi-site 3D T1-weighted 3ÂT magnetic resonance imaging by correcting geometric distortions. Magnetic Resonance Imaging, 2022, 92, 150-160.	1.0	1
123	P4-097: Should a global or a regional measure of amyloidosis be used in a longitudinal study?. , 2015, 11, P811.		0
124	IC-P-011: Comparison of global and voxel-based diagnostic classification using [18 F]florbetapir ROC estimates. , 2015, 11, P18-P19.		0
125	P3-180: Comparison of global and voxel-based diagnostic classification using [18 F]florbetapir ROC estimates. , 2015, 11, P699-P699.		0
126	P4-073: A quantitative comparison between two manual hippocampal segmentation protocols. , 2015, 11, P797-P798.		0

#	Article	IF	CITATIONS
127	O5-01-06: Baseline CSF p-tau and fibrillary amyloid load predict mesial temporal hypometabolism in 24 months' follow-up in cognitively normal subjects. , 2015, 11, P314-P315.		0
128	976. Estradiol, Cortico-Amygdalar Structural Networks and Cognitive Development. Biological Psychiatry, 2017, 81, S395.	0.7	0
129	F67. Increased Amygdalar Activation to Angry Faces is Linked to Reduced Prefrontal Cortical Thickness and Hyperactive/Inattentive Symptomatology in Adolescents. Biological Psychiatry, 2018, 83, S263-S264.	0.7	0
130	A New Framework for Analyzing Structural Volume Changes of Longitudinal Brain MRI Data. Lecture Notes in Computer Science, 2012, , 50-62.	1.0	0